

Supplementary Information for

**Hollow carbon nanospheres dotted with Gd-Fe nanoparticles for
magnetic resonance and photoacoustic imaging**

Hui Zhang,^a Tianze Wu,^a Yi Chen,^a Qianqian Zhang,^a Zhenxia Chen,^a Yun Ling,^{*a,b} Yu Jia,^a Yongtai Yang,^a Xiaofeng Liu,^a and Yaming Zhou^{*a}

^a Shanghai Key Laboratory of Molecular Catalysis and Innovative Materials,
Department of Chemistry, Fudan University, Shanghai, 200433, China.

^b Zhuhai Fudan Innovation Institute, Zhuhai, Guangdong, 519000, China.

*E-mail: yunling@fudan.edu.cn (Prof. Dr. Ling Y.)

ymzhou@fudan.edu.cn (Prof. Dr. Zhou Y. M.)

Table S1. Synthetic parameters for controlling the size and/or thickness of SiO₂@RF.

Sample	TEOS (mL)	EtOH (mL)	H ₂ O (mL)	Resorcinol (g)	HCHO (mL)	Size (nm)	Thickness (nm)
i	0.85	50	3	0.2	0.28	100±10	10
ii	0.85	50	3	0.05	0.07	140±10	10
iii	0.85	35	3	0.2	0.28	200±10	35
iv	0.85	50	3	0.4	0.56	220±10	50
v	0.85	25	3	0.2	0.28	320±10	70

Table S2. A summary information of Gd-Fe/HCSs and HCSs (100 nm).

Sample	Fe (wt %)	Gd (wt %)	r_1 ($\text{mM}^{-1}\cdot\text{s}^{-1}$)	r_2 ($\text{mM}^{-1}\cdot\text{s}^{-1}$)	BET surface area ($\text{m}^2\cdot\text{g}^{-1}$)	τ_s	η
HCSs	/	/	/	/	597	538.15	27.03%
Gd- Fe/HCSs	0.597	1.638	3.78	257.48	481	415.12	35.30%

Fig. S1 FT-IR absorption spectra of $\text{SiO}_2@\text{RF}$, $\{\text{Fe}_6\text{Gd}_6\text{P}_6\}$, $\text{SiO}_2@\text{RF}-\{\text{Fe}_6\text{Gd}_6\text{P}_6\}$, HCSSs, and Gd-Fe/HCSSs. (b) The as-made $\text{SiO}_2@\text{RF}$ composites are homogeneously dispersed in the EtOH solution containing $\{\text{Fe}_6\text{Gd}_6\text{P}_6\}$.

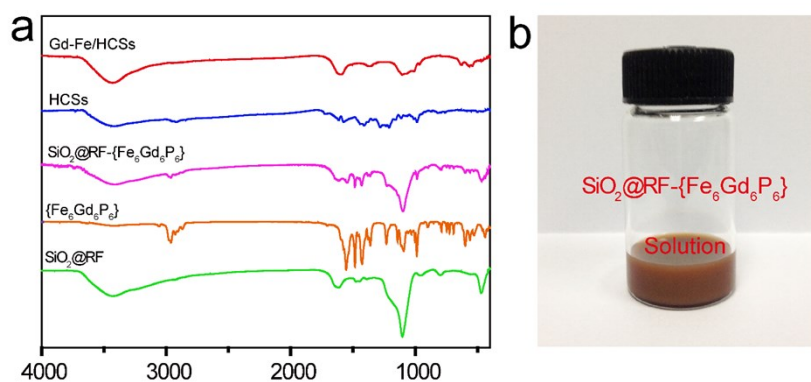


Fig. S2 (a-b) N₂ sorption isotherm of Gd-Fe/HCSs and the corresponding pore size distribution by BJH). (c-d) N₂ sorption isotherms of hollow carbon spheres (HCSs) and the corresponding pore size distribution by BJH, (e-f) N₂ sorption isotherms of core-shell SiO₂@carbon nanospheres (SiO₂@C) and the corresponding pore size distribution by BJH.

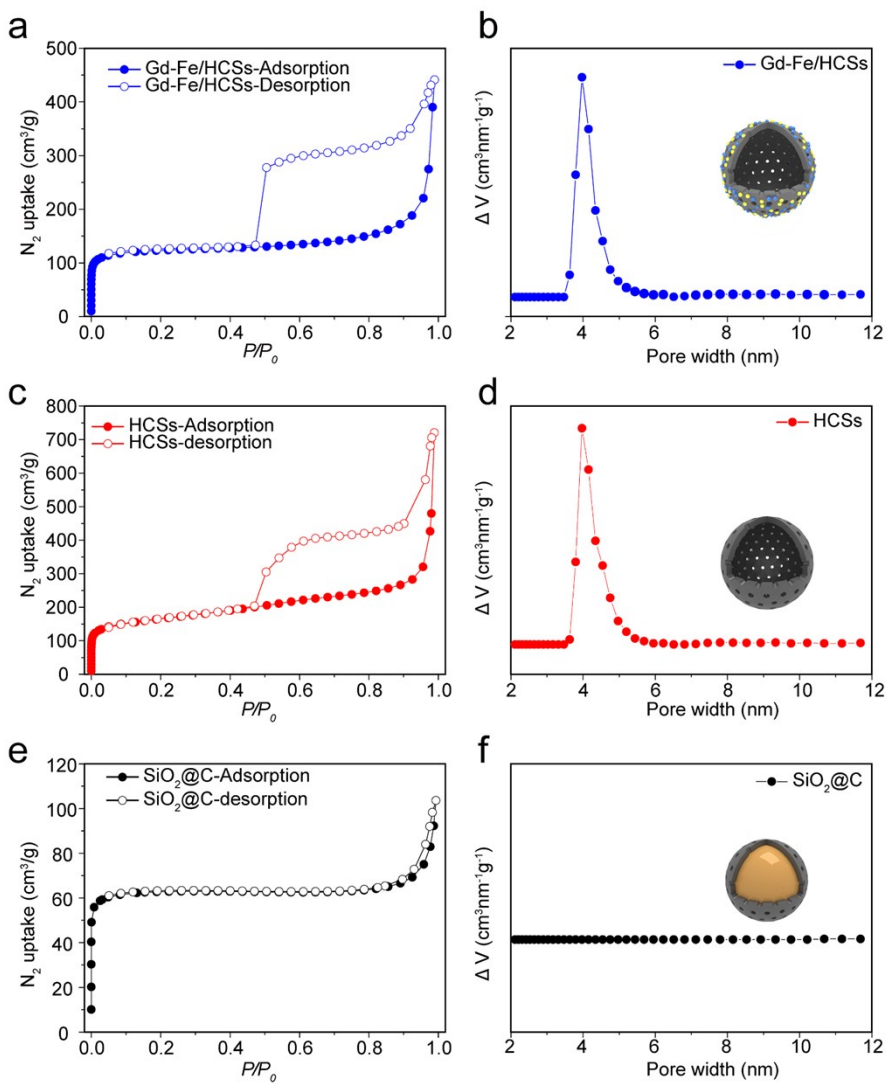


Fig. S3 Raman spectrum of Gd-Fe/HCSs and HCSs.

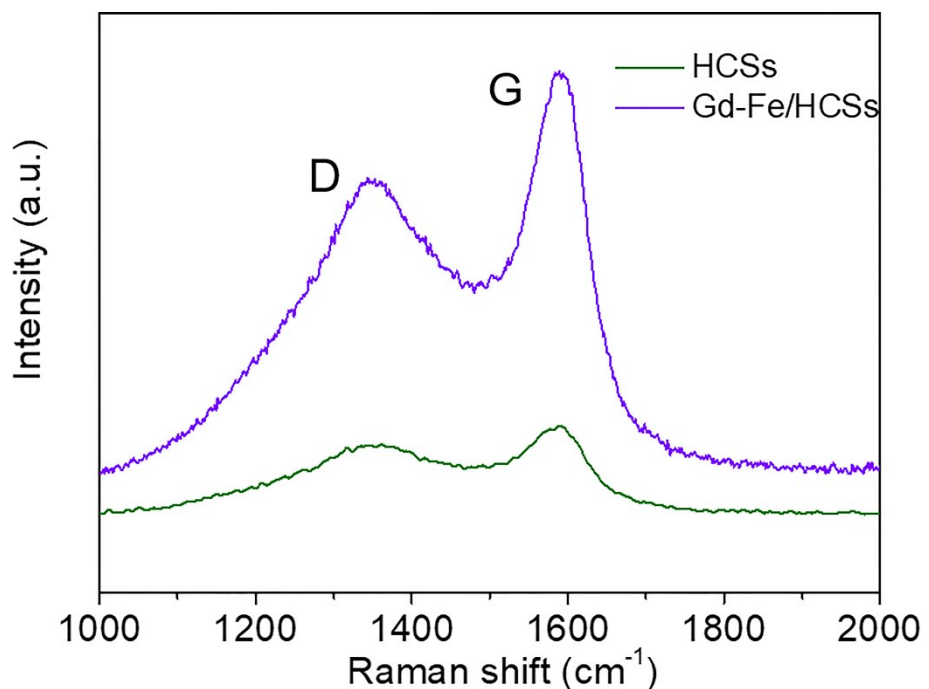


Fig. S4 (a) High-resolution TEM images. Typical lattice fringes are labeled, assigned to the characteristic lattice plane distance of GdPO₄ (red circle) and γ -Fe₂O₃ (yellow circle) (Gd-Fe), and (b) the corresponding element analysis result of Gd-Fe/HCSs, which the Gd/Fe molar ratio is measured close to 1: 1.

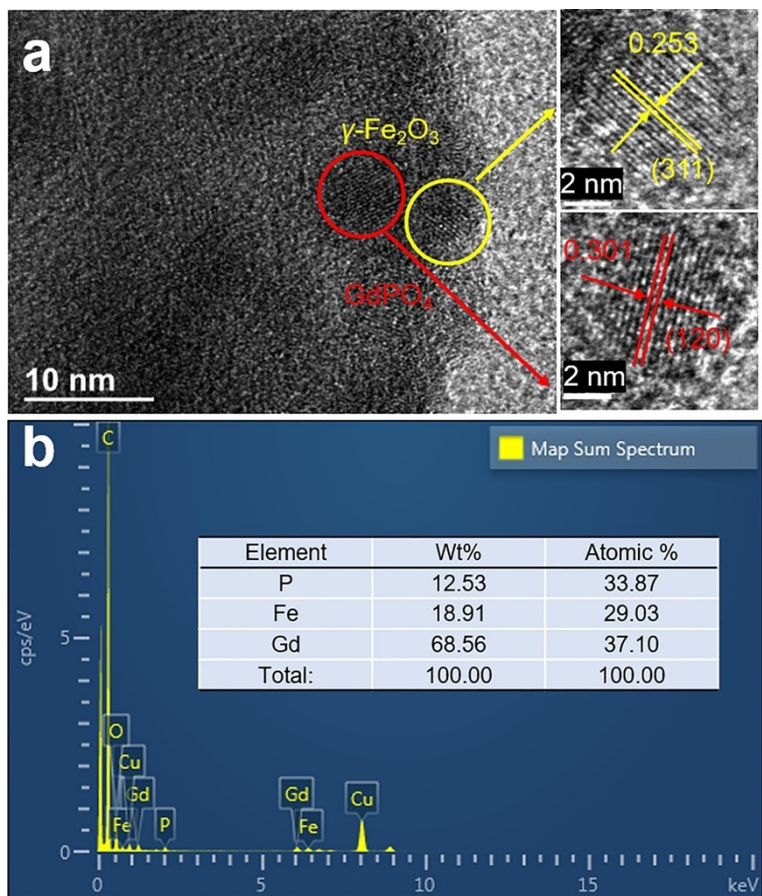


Fig. S5 PXRD patterns of Gd-Fe/HCSs, GdPO_4 (JCPDS card no. 32-0386), and $\gamma\text{-Fe}_2\text{O}_3$ (JCPDS card no. 39-1346).

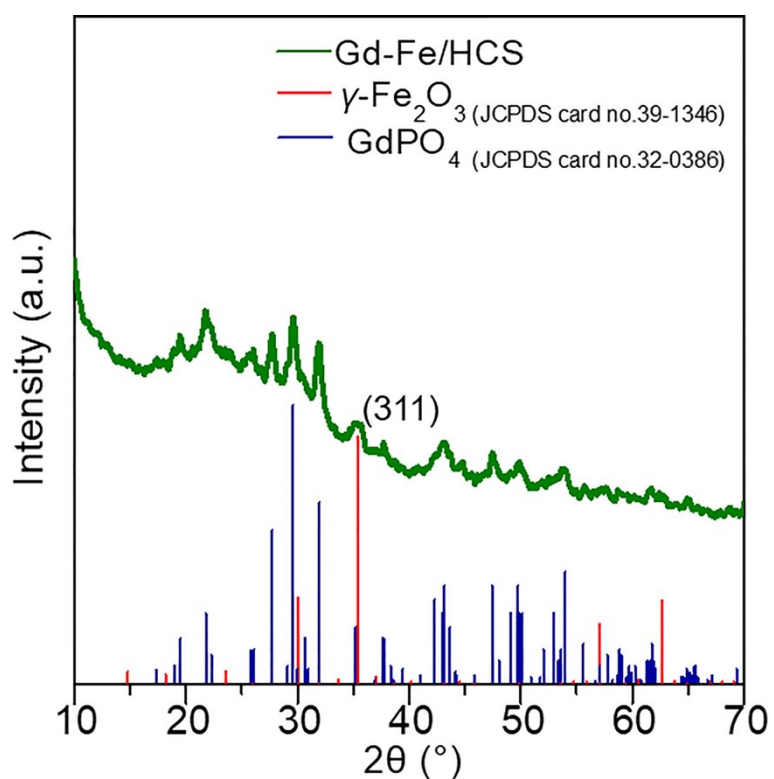


Fig. S6 (a) TEM image, (b-c) HAADF-STEM images, (d-i) overlay maps f C, O, Gd, Fe and P elements, the corresponding EDS maps of C, O, Fe, Gd, P, and EDS line profiles of the {Gd-Fe}/{SiO₂@C}.

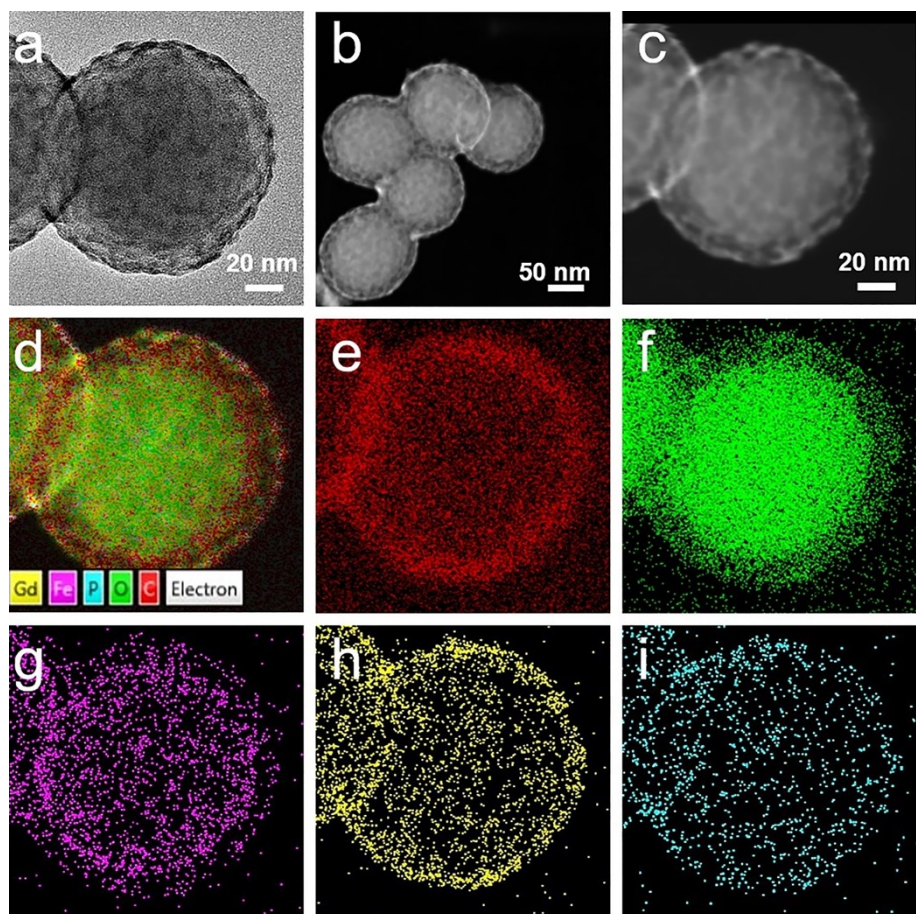


Fig. S7 (a) TEM image, (b-h) HAADF-STEM images, overlay maps of C, O, Gd, Fe and P elements, the corresponding EDS maps of C, O, Fe, Gd, P, and EDS line profiles of the Gd-Fe/HCSs.

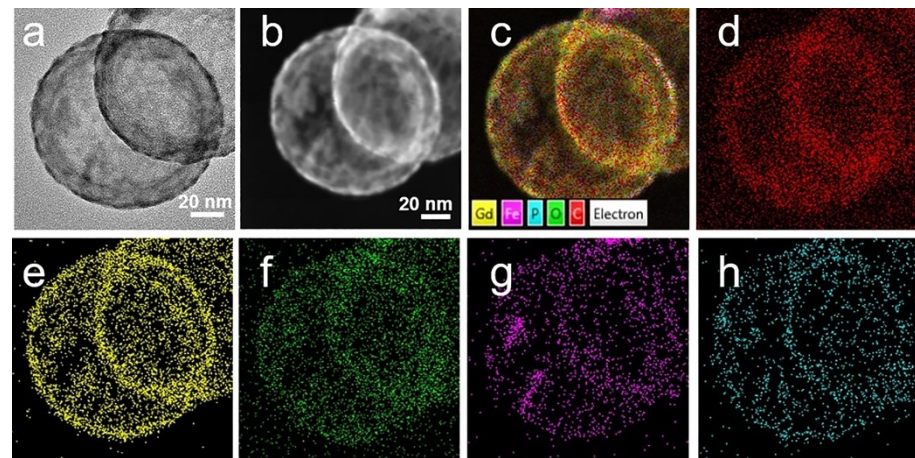


Fig. S8 A view of the different size and thickness of $\text{SiO}_2@\text{RF}$. (a-i) Shell thickness controlled by regulating the addition of resorcinol and HCHO. The corresponding shell thickness in a-i are 10 nm, 35 nm and 50 nm, respectively. (j-l) Size controlled by regulating the addition of EtOH. The corresponding particle sizes in j-l are 310 ± 10 nm and the shell thickness are 70 nm.

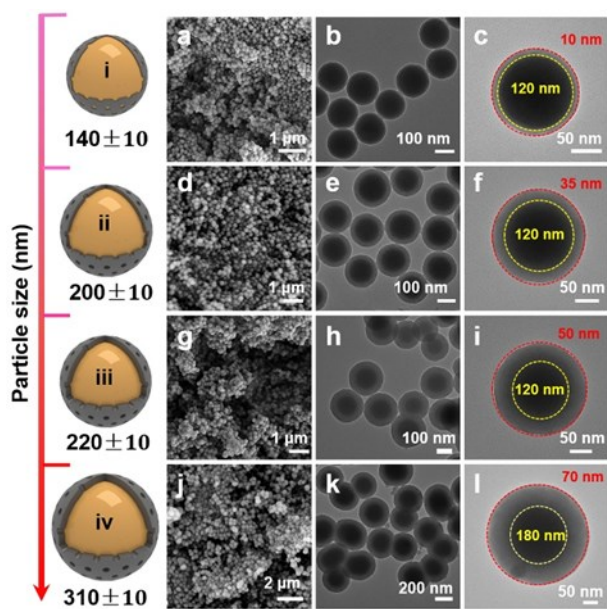


Fig. S9 TEM images of hollow carbon nanospheres with different metal loading (Gd-Fe/HCSs-n, n: the amount of $\{\text{Fe}_6\text{Gd}_6\text{P}_6\}$, n = 0 mg, 1 mg, 3 mg, 6 mg, 12 mg, 18 mg) of 100 nm: (a) HCSs, (b) Gd-Fe/HCSs-1, (c) Gd-Fe/HCSs-3, (d) Gd-Fe/HCSs-6, (e) Gd-Fe/HCSs-12, (f) Gd-Fe/HCSs-18 (100 nm).

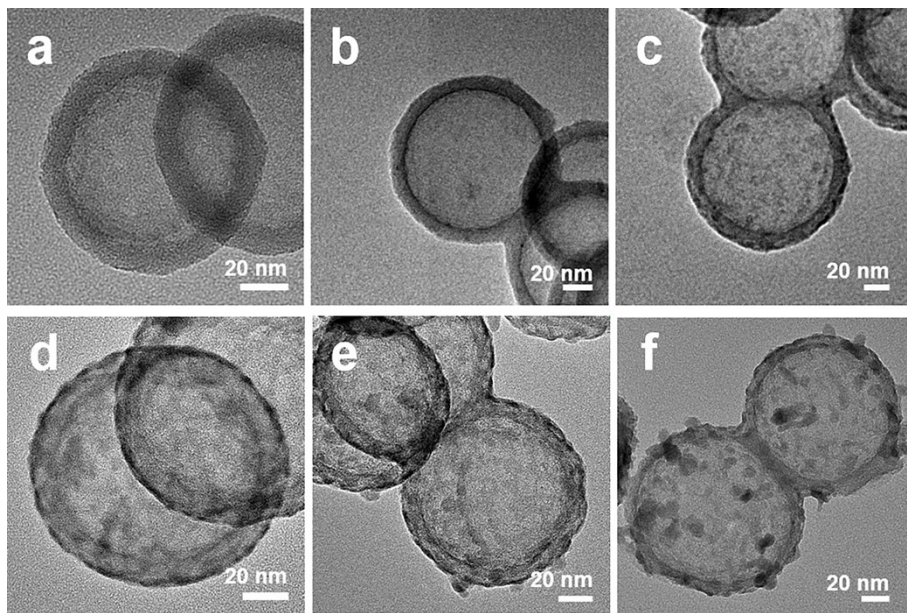


Fig. S10 TEM images of hollow carbon nanospheres with different metal loading (Gd-Fe/HCSs-n) of 320 nm: (a) HCSs, (b) Gd-Fe/HCSs-1, (c) Gd-Fe/HCSs-3, (d) Gd-Fe/HCSs-6, (e) Gd-Fe/HCSs-12, (f) Gd-Fe/HCSs-18 (320 nm).

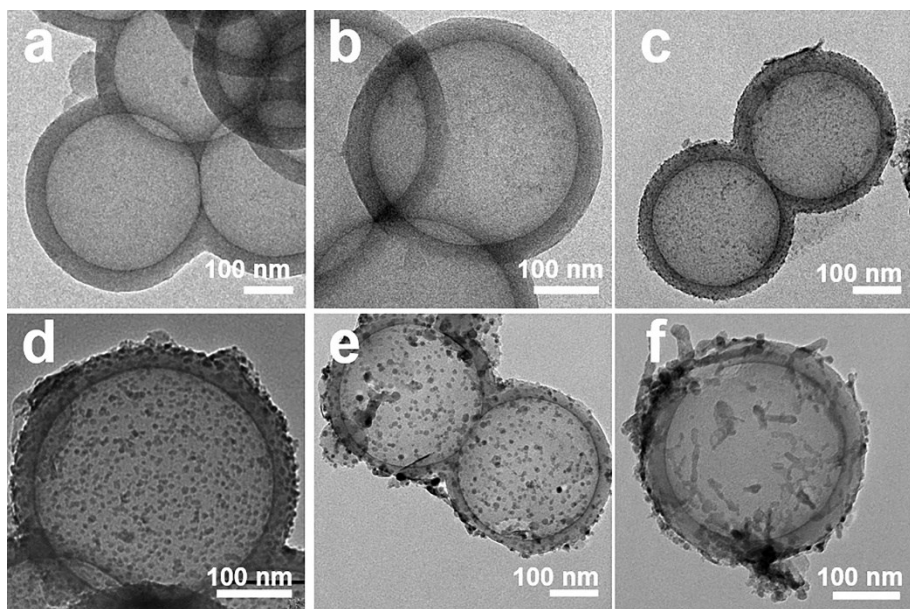


Fig. S11 PXRD patterns of Gd-Fe/HCSs-n ($n = 0$ mg, 1 mg, 3 mg, 6 mg, 12 mg, 18 mg) (320 nm).

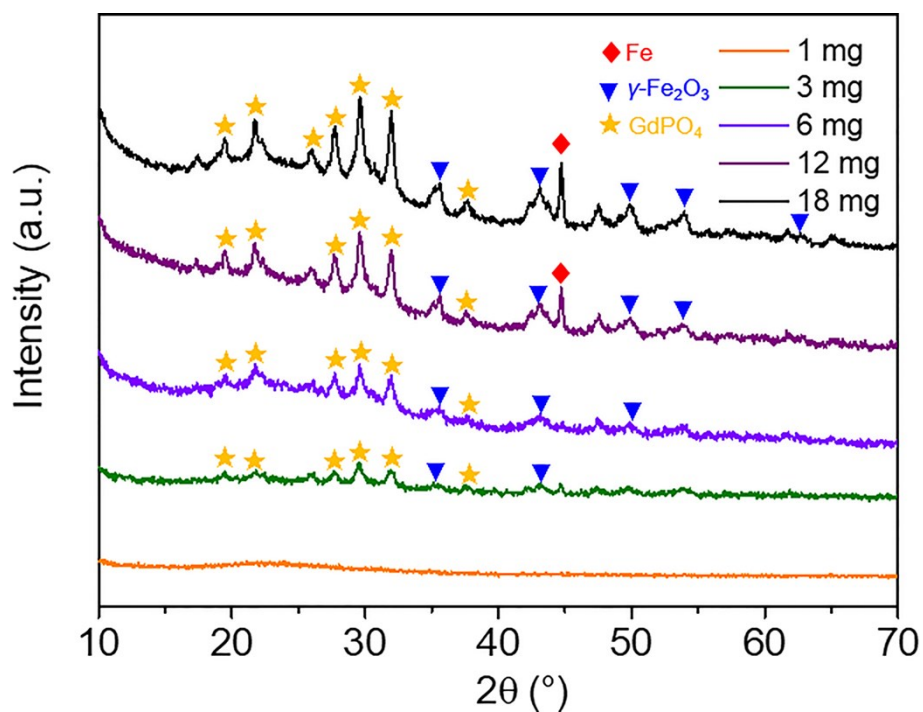
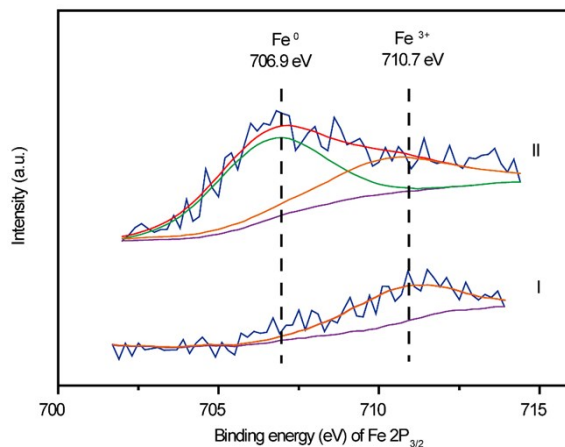


Fig. S12 Fe 2p XPS spectra of the Gd-Fe/HCSs-6 (I) and Gd-Fe/HCSs-18 (II).



As identified by TEM images (Fig. S10), the structure of hollow carbon spheres can be well retained when the dosage changes from 1 mg to 6 mg. Non-aggregation on the shell of hollow carbon spheres and good dispersion of nanoparticles indicates that GdPO₄ and γ -Fe₂O₃ nanoparticles are homogeneously dotted in the shell of HCSs. When the dosage increasing to 18 mg, the aggregation of particles can be observed (Fig. S9). The detectable peak at $2\theta = 44.6^\circ$ could be assigned the characteristic diffraction of the (110) plane of Fe⁰ (Fig. S11), which if further identified by XPS (Fig. S12). This Fe⁰ indicates the occurrence of a redox reaction between carbon and γ -Fe₂O₃.

Fig. S13 The magnetic hysteresis loop of Gd-Fe/HCSs.

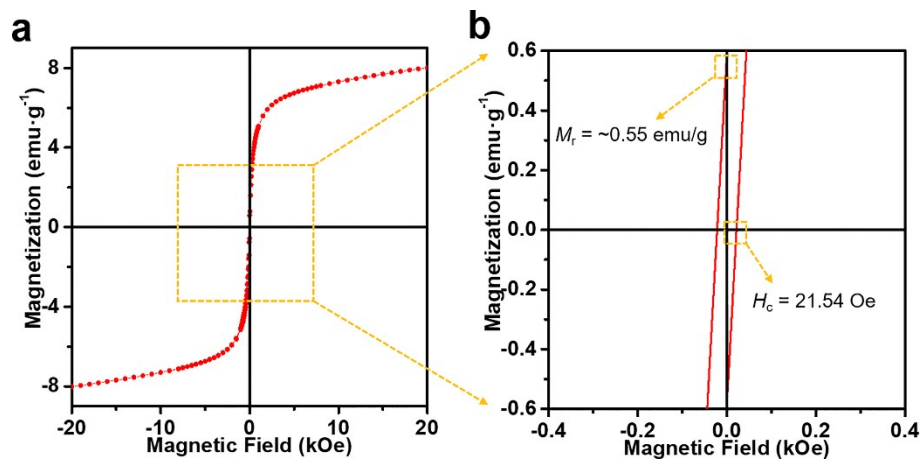


Fig. S14 Uv-vis-NIR absorbance spectra of HCSs and Gd-Fe/HCSs powders.

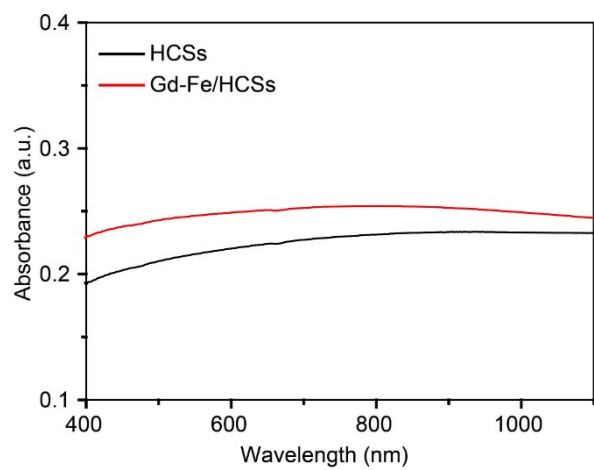


Fig. S15 (a) Uv-vis-NIR absorbance spectra of HCSs and Gd-Fe/HCSs (25, 50, and 100 $\mu\text{g}\cdot\text{mL}^{-1}$).

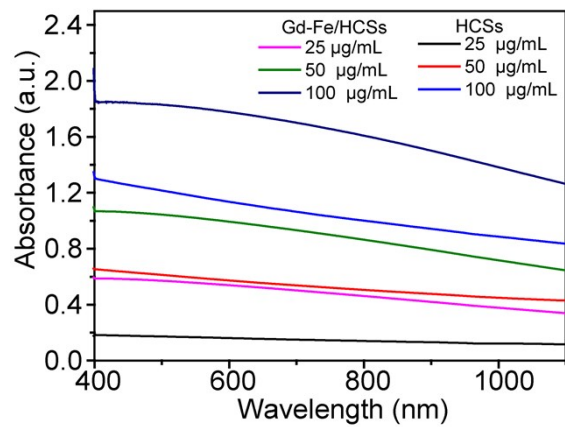


Fig. S16 The optical photograph of the infrared thermographic camera.



Fig. S17 Photothermal conversion characterizations of Gd-Fe/HCSs aqueous solution

with various concentrations under 1.0 W cm^{-2} 808 nm laser irradiation for 10 min.

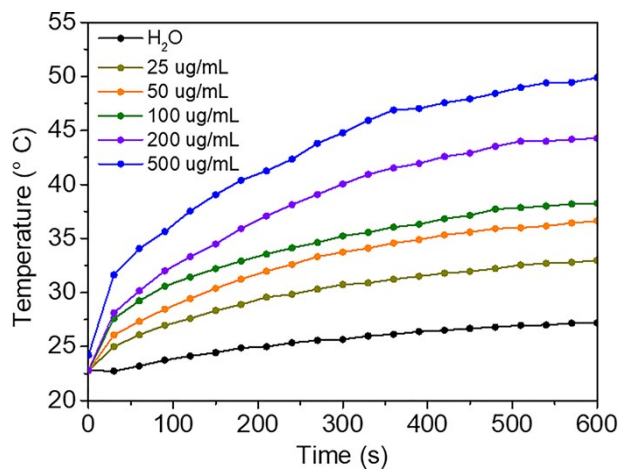


Fig. S18 Linear time data versus $-\ln(\theta)$ obtained from the cooling period of HCSs aqueous solution.

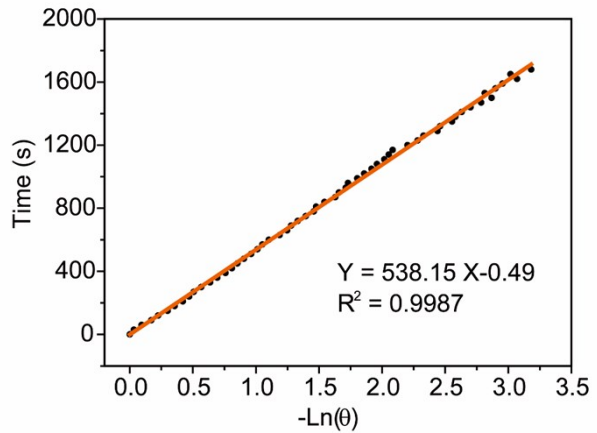


Fig. S19 The viability of HeLa cells after incubated with Gd-Fe/HCSs at different concentrations.

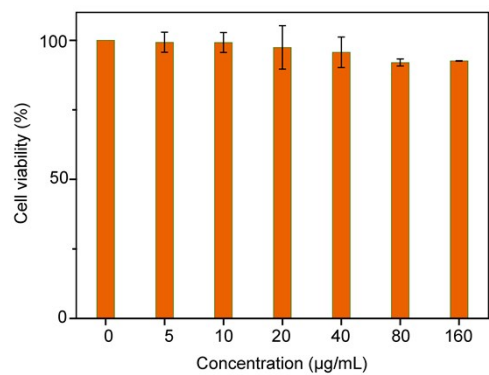


Fig. S2 The experimental setup for the CO_2 absorption measurement *in vitro*.

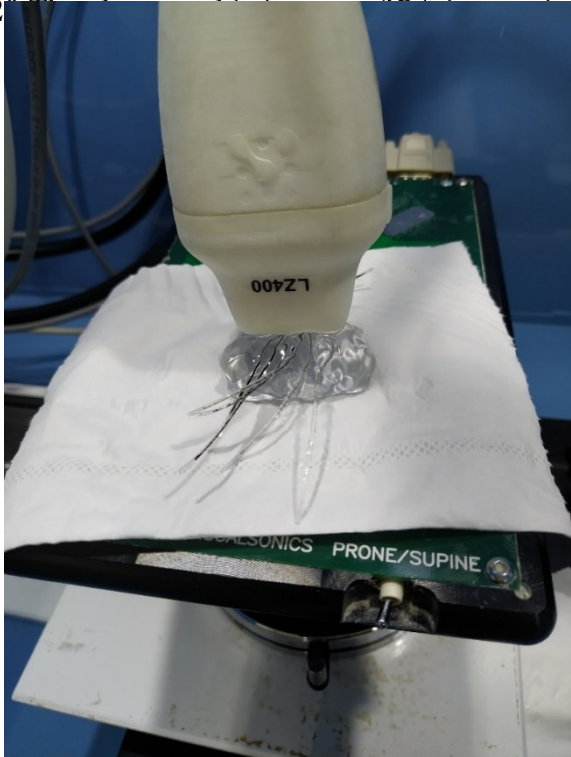


Fig. S21 (a) In vitro PA signals and (b) the corresponding PA signal intensities of HCSs with different concentrations.

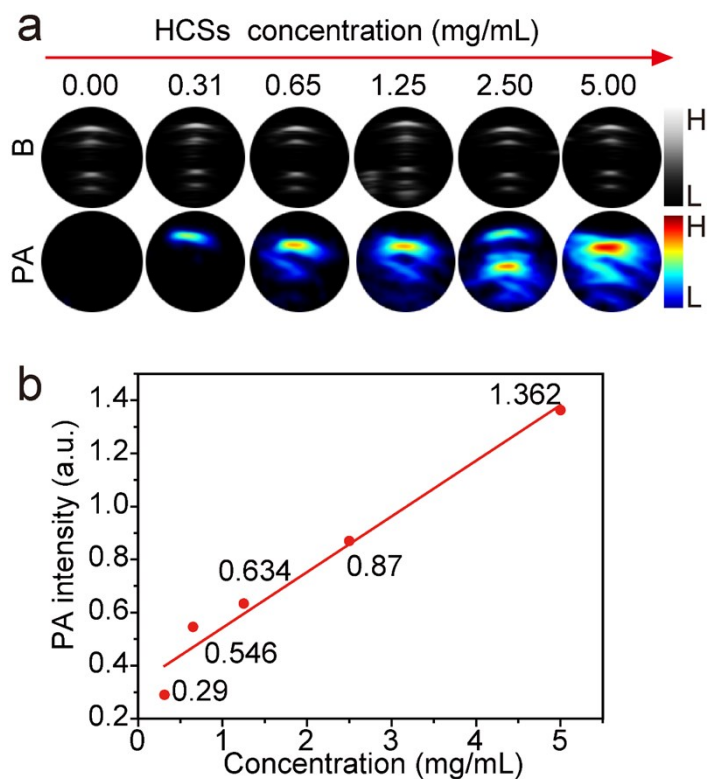


Fig. S22 (a) The optical images of the HCSs and Gd-Fe/HCSs aqueous solutions. (b) The size distribution of Gd-Fe/HCSs and (c) the zeta-potential of Gd-Fe/HCSs, and (d) the zeta-potential of HCSs.

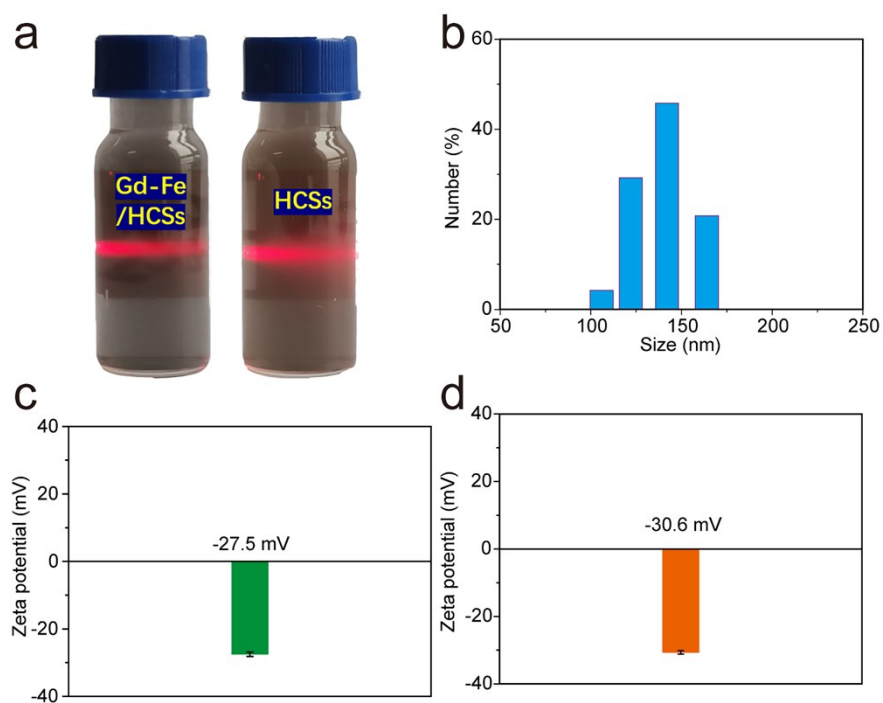


Fig. S23 (a) In vivo PA images and (b) the corresponding PA intensities of liver at different time points of HCSs (pre, 0.25 h, 1 h, 4 h, and 24 h).

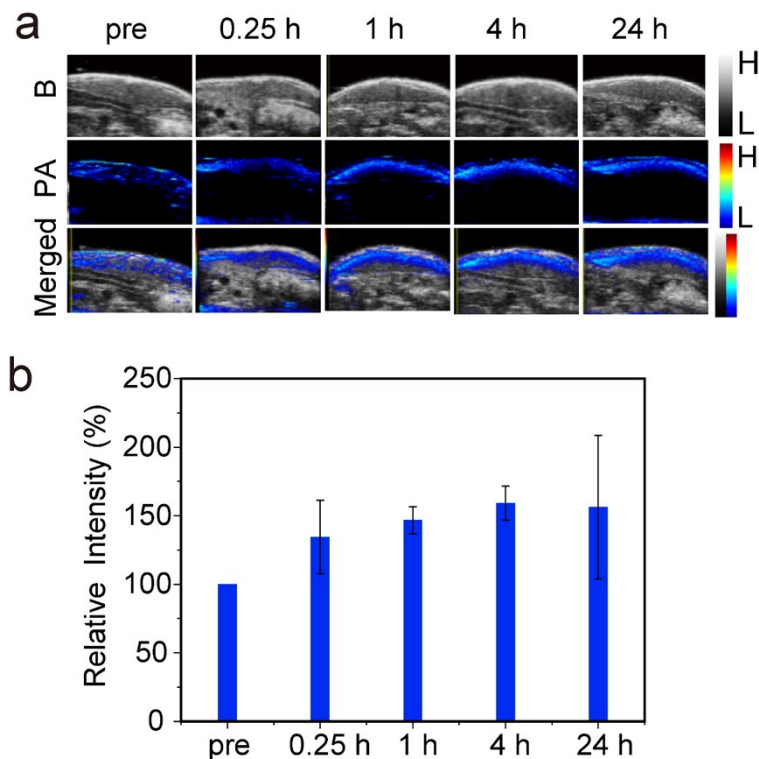


Fig. S24 Hematoxylin and eosin (H&E) images of major organs collected from mice treated with saline, and Gd-Fe/HCSs.

